CHEMISTRY
A EUROPEAN JOURNAL

DOI: 10.1002/chem.200903096

Preparation and Characterization of a Bifunctional Aldolase/Kinase Enzyme: A More Efficient Biocatalyst for C–C Bond Formation

Laura Iturrate,[a] Israel Sánchez-Moreno,[a] Isabel Oroz-Guinea,[a] Jesús Pérez-Gil,[b] and Eduardo García-Junceda*[a]

Abstract: A bifunctional aldolase/kinase enzyme named DLF has been constructed by gene fusion through overlap extension. This fusion enzyme consists of monomeric fructose-1,6-bisphosphate aldolase (FBPA) from *Staphylococcus carnosus* and the homodimeric dihydroxyacetone kinase (DHAK) from *Citrobacter freundii* CECT 4626 with an intervening linker of five amino acid residues. The fusion protein was expressed soluble and retained both kinase and aldolase activities. The secondary structures of the bifunctional enzyme and the parental enzymes were analyzed by circular dichroism (CD) spectroscopy to study the effect of the covalent coupling of the two parent proteins on the structure of the fused enzyme. Because *S. carnosus* FBPA is a thermostable protein, the effect of the fusion on the thermal stability of the bifunctional enzyme has also been studied. The proximity of the active centers in the fused enzyme promotes a kinetic advantage as the 20-fold increment in the initial velocity of the overall aldol reaction indicates. Experimental evidence supports that this increase in the reaction rate can be explained in terms of substrate channeling.

Keywords: aldolases · biocatalysis · circular dichroism · fusion enzymes · protein engineering

Introduction

The aldol addition reaction has long been recognized as one of the most useful tools that has the synthetic chemist for the construction of new carbon–carbon bonds.[1] Concomitant with the C–C bond-forming process is the formation of one or two new stereocenters, which allows an approach toward the synthesis of a broad range of both natural and novel compounds. Aldolases are among the most important biocatalysts used in Nature for C–C bond formation. Dihydroxyacetone (DHA) phosphate-dependent aldolases have been thoroughly used to synthesize carbohydrates, carbohydrate-like structures, or non-carbohydrate compounds.[2] Their major synthetic advantage is that the stereochemistry of the two newly formed stereogenic centers is controlled by the enzymes, and moreover they are stereocomplementary, in that they can synthesize the four possible diastereoisomers of vicinal diols from achiral aldehyde acceptors and dihydroxyacetone phosphate (DHAP). However, it is also well known that their major drawback is their strict specificity for DHAP. Besides the limitation in scope that this fact represents, DHAP is expensive to be used stoichiometrically in large-scale synthesis and is labile at neutral and basic pH values, thus meaning that its effective concentration diminishes with time in the enzymatic reaction media. Efforts to overcome the DHAP dependence of aldolases have involved the formation in situ of arsenate or borate esters of DHA, which act as phosphate ester mimics;[3] the use of enzyme-directed evolution strategies to modify their donor–substrate specificity;[4] the development of catalytic antibodies and small peptides with aldolase activity;[5] de novo design of retro-aldol enzymes;[6] and the use of newly discovered enzymes.[7] Besides these efforts, an efficient method of DHAP preparation is still essential and several chemical and enzymatic routes toward DHAP synthesis have been described.[8] With respect to chemical synthesis, starting from the DHA dimer[9] or 1,3-dibromoacetone[10]

[a] Dr. L. Iturrate, Dr. I. Sánchez-Moreno, I. Oroz-Guinea, Dr. E. García-Junceda
Departamento de Química Bioorgánica
Instituto de Química Orgánica General, CSIC
Juan de la Cierva 3, 28006, Madrid (Spain)
Fax: (+34) 915-644-853
E-mail: eduardo.junceda@iqog.csic.es

[b] Dr. J. Pérez-Gil
Departamento de Bioquímica y Biología Molecular
Facultad de Biología, Universidad Complutense
28040 Madrid (Spain)

Supporting information for this article is available on the WWW under http://dx.doi.org/10.1002/chem.200903096.

provides a stable precursor of DHAP. On the other hand, the enzymatic preparation of DHAP is usually coupled with the aldol condensation catalyzed by aldolase. Thus, DHAP can be prepared by oxidation of L-glycerol 3-phosphate (L-G3P) catalyzed by glycerophosphate oxidase, coupled with hydrogen peroxide decomposition by catalase.[11] Later on, this multienzyme system was coupled with the preparation of D,L-G3P in situ either by phosphorylation of glycerol catalyzed by phosphatase phytase[12] or by the regioselective opening of the *rac*-glycidol epoxide ring with phosphate.[13] A cascade reaction for the generation of DHAP in situ by using the acid phosphatase from *Shigella flexneri* and pyrophosphate (PP_i) as a phosphoryl donor has also been described.[14] Direct kinase-catalyzed phosphorylation of DHA that uses adenosine 5′-triphosphate (ATP) as the phosphoryl donor constitutes another strategy to obtain DHAP. This approach was first described in 1983 by Wong and Whitesides and used the enzyme glycerol kinase.[15] Yeast ATP-dependent dihydroxyacetone kinases (DHAKs) have also been used for the simple and efficient preparation of DHAP.[16]

Our research group has developed a straightforward multienzyme system for a one-pot C–C bond-formation procedure catalyzed by DHAP-dependent aldolases that allows the use of DHA as the initial donor. This system is based on the use of the recombinant ATP-dependent DHAK from *C. freundii* CECT 4626 for the phosphorylation of DHA in situ.[17] This enzyme has the highest catalytic efficiency for the phosphorylation of DHA reported.[18] The multienzyme system was completed with the regeneration of ATP catalyzed by acetate kinase (Scheme 1). This multienzyme system is attractive because it is a one-pot/one-step route to the phosphorylated aldol adduct, and we have shown its utility with three synthetically useful DHAP-dependent aldolases and with a great variety of commercially available aldehydes.[17]

However, there are at least two aspects that can be optimized: First, the number of enzymes that take part on the system. Although the different enzymes can be overproduced in recombinant organisms, the purification of proteins is widely recognized as technically and economically challenging, thus accounting for a substantial fraction of the total manufacturing cost and becoming one of the limiting steps in bioprocess development.[19] Second, the high sensitivity of the ATP regeneration system to pH level and organic solvents.[17b]

Herein, we offer an approach to solve the first point. One way to decrease the number of enzymes that express and purify is to splice two or more enzymatic activities in only one polypeptide, thus creating a hybrid or fusion enzyme.[20] Fusion proteins have great number of applications in biotechnology, which range from analytical procedures[21] to metabolic engineering,[22] with the purification of proteins as the main application.[23] The use of fusion proteins in biotransformation may have other even more interesting effects due to the physical association of enzymes that catalyze sequential reactions into covalently linked complexes. The proximity of the active sites of two enzymes in multienzyme complexes can provide a substantial contribution from substrate channeling in addition to the random diffusion path.[24] Some of the potential catalytic advantages of substrate channeling include: 1) a decrease in the transit time required for an intermediate to reach the active site of the subsequent enzyme; 2) a reduction in the transient time for the system to reach the new steady state; 3) protection of chemically labile intermediates; 4) circumvention of unfavorable equilibria and kinetics imposed by bulk-phase metabolite concentrations; and 5) segregation of the intermediates from competing chemical and enzymatic reactions.[24,25] In spite of these numerous potential advantages, fusion enzymes have been scarcely used in the biotransformation field.[26]

Herein, we have engineered a bifunctional enzyme (named DLF), which joins aldolase and kinase activities in the same polypeptide.[27] We describe the design, expression, and structural and functional characterization of this new biocatalyst.

Results and Discussion

Design of the fused aldolase/kinase enzyme: A key point when designing a fusion protein is the consideration of the possible interactions between the subunits that can take place in the context of the chimera. When two monomeric proteins are fused, it is expected that the resultant fusion protein retains the monomeric character of the parent enzymes. However, if the parent proteins have a dimeric or oligomeric character, the quaternary structure of the fusion protein is difficult to predict and macromolecular complexes of different size and activities may be formed (Scheme 2).[20a]

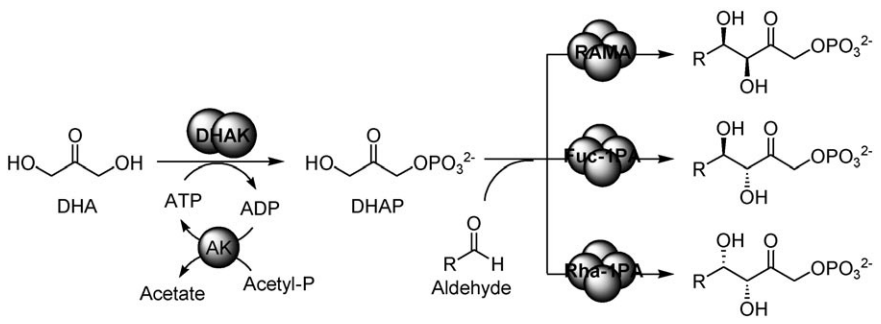

Scheme 1. Multienzyme system for C–C bond formation catalyzed by DHAP-dependent aldolases based on the phosphorylation of DHA in situ catalyzed by DHAK from *C. freundii*. ADP = adenosine diphosphate.

As DHAK from *C. freundii* is a dimeric enzyme,[28] we have chosen the fructose-1,6-bisphosphate aldolase (FBPA) from *Staphylococcus carnosus* as aldolase partner because of its

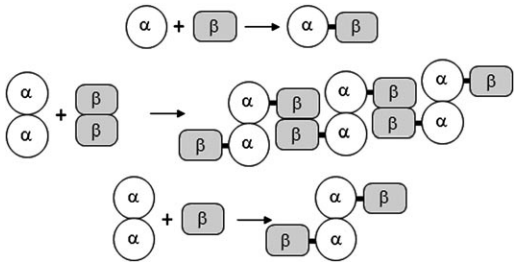

Scheme 2. Representation of the quaternary structure that can acquire a fused protein depending on the oligomeric nature of the parental proteins (adapted from ref. [20a]).

monomeric structure.[29] This aldolase belongs to class I, the reaction mechanism of which proceeds through the formation of a Schiff base intermediate between the donor substrate and a highly conserved lysine residue in the active site of the enzyme. In addition, this aldolase has a high stability toward pH and temperature.[29a] Kula and co-workers postulate that both stabilities are a result of the monomeric structure and of a high renaturation potential. The crystal structure of FBPA from *S. carnosus* is unknown but the protein has a high degree of identity (55%) with the enzyme from *Porphyromonas gingivals*, the crystal structure of which has been resolved.[29] Figure 1 represents the 3D structure of FBPA from *S. carnosus* modeled by the SWISS-MODEL server,[31] which uses the structure of the enzyme from *P. gingivals* as a template.

Figure 1. Three-dimensional structure of the FBPA from *S. carnosus* modeled by the SWISS-MODEL server. The putative catalytic lysine is shown as a ball-and-stick representation.

Another key point in the design of a fusion protein is the selection of the linker sequence. Linker length and sequence composition can affect the folding and activity of the chimeric protein. The linker sequence that has been selected to join the aldolase and the kinase enzymes was designed with the aid of the LINKER program.[32] The linker has to be long enough and sufficiently flexible to allow proper folding of each protein domain but short enough to keep the active sites close to invigorate possible substrate-channeling effects. In this sense, sequences with a preference for adopting an extended conformation are more desirable than sequences with a high propensity to adopt α-helix or β-strand structures, which could limit the flexibility of the system. We arbitrarily fixed a length of five amino acids for the linker sequence, and a series of sequence filters, such as the absence of polar, charged, or hydrophobic residues, were introduced in the LINKER program. With this input, the LINKER program automatically generated a set of three peptide sequences known to adopt extended conformations (Figure 2). The sequence Gln-Gly-Gln-Gly-Gln (Gln = glutamine, Gly = glycine) was chosen because the DNA coding sequence does not contain restriction sites for the enzymes *Xho*I and *Nde*I chosen for the cloning of the fusion enzyme. The sequence is flexible to allow the native folding of the fused enzymes and short enough to keep the kinase and aldolase active centers close.

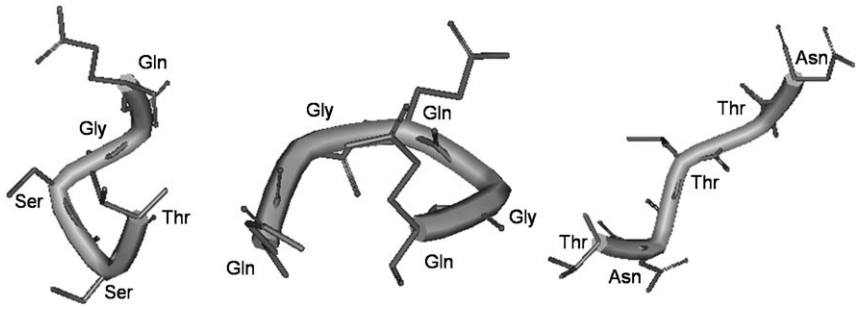

Figure 2. Three-dimensional structure of the three peptide sequences generated by the LINKER program. The structure shown is the one that these peptides present in the context of their corresponding protein. Asn = asparagine, Ser = serine, Thr = threonine.

Finally, because the C-terminal of FBPA is closer to the active center than the N-terminal, we decided to carry out the fusion through this end. Therefore, the designed construction of the new bifunctional enzyme was DHAK-linker-FBPA (Scheme 3).

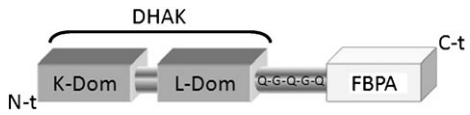

Scheme 3. Disposition of the different elements in the designed bifunctional aldolase/kinase enzyme DLF. C-t = C-terminal, K-Dom = K domain, L-Dom = L domain, N-t = N-terminal.

Construction and characterization of the bifunctional DLF enzyme: The genes *dhak* from *C. freundii* and *fda* from *S. carnosus* were 'spliced' together by overlap extension to construct the bifunctional DLF enzyme.[33] This method

comprises two polymerase chain reaction (PCR) steps. In the first PCR step, the *dhak* and *fda* genes were amplified separately including sites for the restriction enzymes *Nde*I (5′-*dhak*) and *Xho*I (3′-*fda*). Extremes 3′-*dhak* and 5′-*fda* included the 15 nucleotides that code for the linker sequence (*l*). These amplified genes were used as templates in a second PCR step (Figure 3).

The construction *dhak-l-fda* (2565 bp) was cloned into the pET-28b(+) expression vector that include a N-terminal histidine tag that extended the recombinant protein. Analysis with sodium dodecyl sulfate–polyacrylamide gel electrophoresis (SDS–PAGE) of DLF expression in *E. coli* BL21(DE3) showed that DLF was expressed soluble and represented 75% of the total protein with a productivity of 135 and 425 $U L^{-1}$ of culture broth for the kinase and aldolase activities, respectively (ratio of kinase/aldolase activity was 1:3).

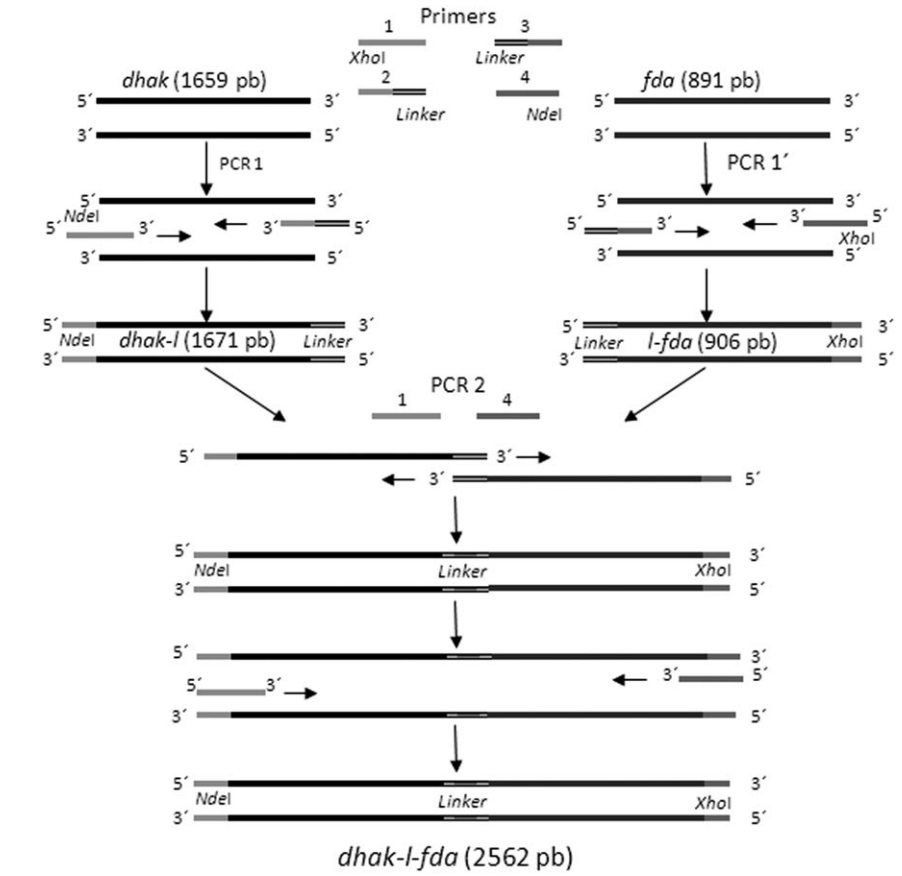

Figure 3. Strategy used for *dhak* and *fda* gene splicing by overlap extension. bp = base pair.

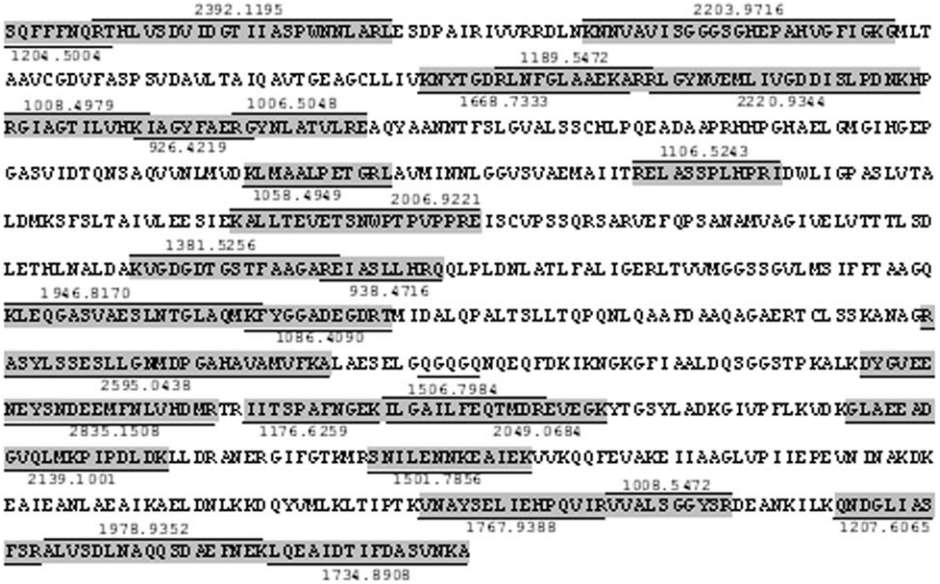

Figure 4. Peptide-mass fingerprint of bifunctional DLF. The sequence of the identified peptides is shaded and underlined. The molecular mass of each peptide is indicated in Da. The linker sequence is underlined.

DLF was purified by immobilized metal affinity chromatography (IMAC) followed by size-exclusion chromatography. Peptide-mass fingerprinting verified that the purified protein had the expected features of DLF. Twenty peptides that covered the DHAK sequence and 13 peptides that covered the FBPA sequence were identified (Figure 4). Sedimentation equilibrium analysis of the purified protein confirmed the expected molecular weight and showed that the fusion protein was a homodimer, such as native DHAK (Figure 5).

To analyze the effect of the covalent coupling of DHAK and FBPA in the fused enzyme, we compared its kinetic behavior and secondary structure with those from the parent enzymes. The kinetic parameters of the DLF enzyme were calculated independently for the phosphorylation of DHA to analyze the kinase activity and for the retro-aldol reaction of fructose-1,6-bisphosphate to

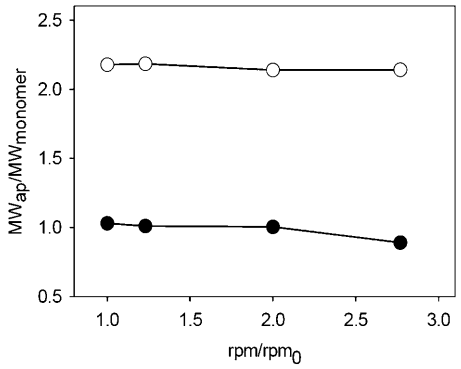

Figure 5. Sedimentation equilibrium analysis of FBPA (●) and DLF (○).

evaluate the aldolase activity. DLF showed a Michaelis–Menten kinetic for both activities, as did the parent enzymes. The covalent union of both enzymes did not substantially modify either the K_M or the k_{cat} values of the DLF aldolase activity (Table 1). On the other hand, both constants were slightly modified for the DLF kinase activity (Table 1). The increase in the K_M values and decrease in k_{cat} values of about threefold results in a loss of catalytic efficiency (k_{cat}/K_M) of the kinase activity in the fusion enzyme of about one order of magnitude. This loss in catalytic efficiency could be a direct result of the entropy loss of the two active sites in the bifunctional enzyme relative to the independent proteins. Apart from this, it cannot be discarded that some active centers of the kinase had lost accessibility for the substrate in the fusion enzyme. However, despite this decrease, the k_{cat}/K_M value for this activity in the fusion enzyme, that is, on the order of 10^6 ($s^{-1}M^{-1}$), is high enough to allow its use in C–C coupling reactions.

Circular dichroism (CD) study of the DLF secondary structure: The far-UV CD spectra obtained for the fused and parent enzymes are indicative of a predominantly α-helical structure with two minima at approximately $\lambda = 208$ and 222 nm (Figure 6a). The contribution of each type of secondary structure is summarized in Table 2.

From the CD spectra of DHAK and FBPA, one can calculate the structural composition of an equimolar mixture of these enzymes [Eq. (1); see the Experimental Section]. The calculated values should match the structural composition of DLF if the fusion has no significant effect on the folding of the fused protein domains. DLF has a contribution of α-helix ($46.2 \pm 1.81\,\%$) slightly lower than expected for the mixture of DHAK and FBPA (Table 2). The CD spectrum of an equimolar mixture of DHAK and FBPA was recorded to determine whether this small difference could be due to the fusion of both enzymes or to unspecific noncovalent interactions between them (Figure 6b). The contribution of each secondary-structure component calculated from the CD spectra of the enzyme mixture agreed with the values

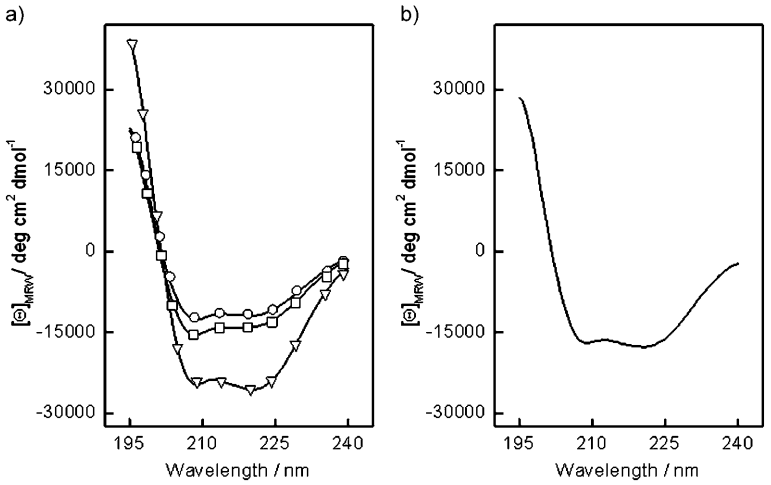

Figure 6. CD spectra at 20°C of a) DHAK (○), FBPA (▽), and DLF (□) and b) equimolar mixture of DHAK and FBPA.

Table 1. Summary of the kinetic constants of the bifunctional DLF and the parent enzymes.

	DHAK[a]	FBPA[b]	DLF kinase	DLF aldolase[b]
K_M [M]	1.22×10^{-6}	1.46×10^{-5}	3.80×10^{-6}	1.88×10^{-5}
k_{cat} [s^{-1}]	24.13	16.76	8.16	20.30
k_{cat}/K_M [$s^{-1}M^{-1}$]	1.98×10^{7}	1.16×10^{4}	1.19×10^{6}	1.08×10^{4}

[a] Constant determined for the phosphorylation of DHA.[18] [b] Constant determined in the retro-aldol reaction with FBP as the substrate.

Table 2. Summary of the contribution of the different secondary structures components in DHAK, FBPA, DLF, and the DHAK/FBPA mixture.[a]

	α-Helix	β-Sheet	Turns	Unordered
DHAK	41.4 ± 0.95	13.2 ± 0.93	16.8 ± 0.46	28.2 ± 1.95
FBPA	67.2 ± 3.16	5.0 ± 2.80	11.4 ± 3.05	17.4 ± 4.20
DLF	46.2 ± 1.81	11.2 ± 0.98	16.2 ± 0.65	26.0 ± 1.54
Mixture[b]				
exptl.[c]	52.7 ± 2.50	8.3 ± 0.46	15.0 ± 1.33	24.7 ± 1.80
calcd[d]	53.39	10.86	15.72	25.75

[a] Contribution of each type of secondary structure is expressed as a percentage. [b] Equimolar DHAK/FBPA mixture. [c] Values obtained from the CD spectra of the DHAK/FBPA mixture. [d] Values calculated applying Equation (1) (see the Experimental Section) to the data obtained for the parent DHAK and FBPA enzymes.

obtained on applying Equation (1) (Table 2). We conclude that the covalent union of both proteins is responsible for this minor reduction in the α-helical conformation.

Is the thermostability of FBPA transferred to the fused DLF enzyme? As commented on previously, FBPA from *S. carnosus* has a considerable thermostability.[29a] Therefore, it was interesting to investigate whether this thermostability has been somehow transferred to the fusion enzyme. The thermal stability of the three enzymes (i.e., DHAK, FBPA, and DLF) was initially assessed by using CD spectroscopic analysis, in which temperature dependence of the dichroism signal at $\lambda = 222$ nm was monitored (Figure 7). From these curves, the melting temperature (T_m) of the proteins can be calculated if they fit a two-state folding model [Eq. (2); see the Experimental section].[34] The curve following the thermal unfolding of DHAK (Figure 7a) could be fitted to a simple thermodynamic unfolding model. The melting temperature (midpoint of the transition) was determined to be 49.9 ± 0.1 °C. In addition, the transition region was very narrow and sharp, thus indicating that the protein existed initially as a compact, well-folded structure and that the unfolding reaction was highly cooperative. The DLF curve (Figure 7c) also responds to a two-state unfolding model, with a melting temperature of 51.8 ± 0.25 °C, which is significantly higher than the T_m value calculated for DHAK. On the other hand, although somewhat less narrow and sharp than that of the DHAK, the width and shape of the transition region corresponds also to a initially well-folded structure and a cooperative melting process. However, the behavior of FBPA was completely different (Figure 7b). The curve clearly suggested the existence of two transitions, and therefore it did not fit to a simple thermodynamic unfolding model. Hence, we decided to analyze the thermal denaturation of FBPA in terms of "fraction of unfolding" f_u,[35] which is defined herein as the fraction of the total loss of α-helix that has occurred at each particular temperature. For comparative purposes, we applied the same analysis to DHAK and DLF. The T_m value calculated for DHAK and DLF from the temperature dependence of the fraction of unfolding (48.7 and 53.7 °C, respectively) are consistent with the T_m values calculated from the melting curves in Figure 7 (Figure 8). Figure 8 also shows that the melting temperature of the fusion enzyme DLF almost coincides with FBPA (i.e., 54.9 °C).

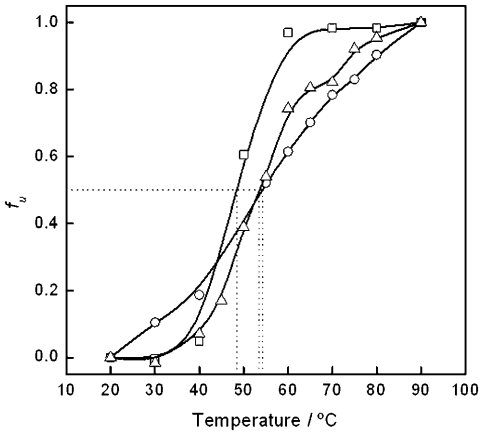

Figure 8. Thermal denaturation profiles of DHAK (□), FBPA (○) and DLF (△).

As we investigated in the study of the secondary structure, we studied the thermal denaturation of an equimolar mixture of DHAK and FBPA (Figure 9) to evaluate if the behavior of the fused enzyme was due to the covalent union of DHAK and FBPA or just due to the simultaneous presence of both proteins. The thermal denaturation of the mixture fits a two-state folding model with a transition region wider than DHAK and DLF, which is consistent with the presence of a heterogeneous population of folded structures. On this occasion, there was a disparity of 5 °C between the T_m value calculated from the CD spectrum at $\lambda = 222$ nm (44.2 ± 0.5 °C; Figure 9a) and the value calculated from the fraction of unfolding (49.3 °C; Figure 9b). Anyway, both values are lower than the T_m value calculated for the fused enzyme (53.7 °C). Therefore, the covalent union of FBPA and DHAK allows the thermostability of FBPA to be trans-

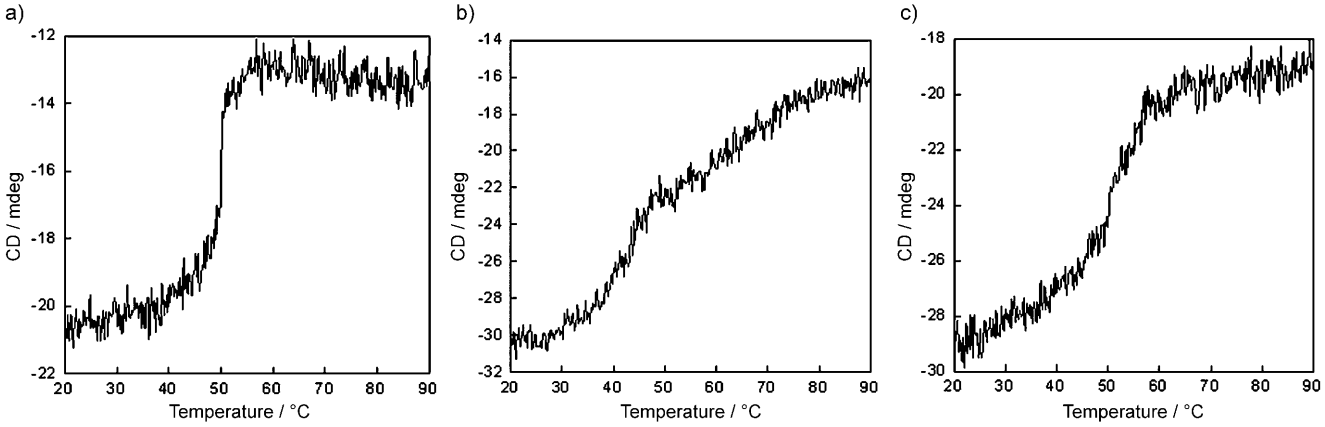

Figure 7. Variation with the temperature of the CD spectra at $\lambda = 222$ nm of a) DHAK, b) FBPA, and c) DLF.

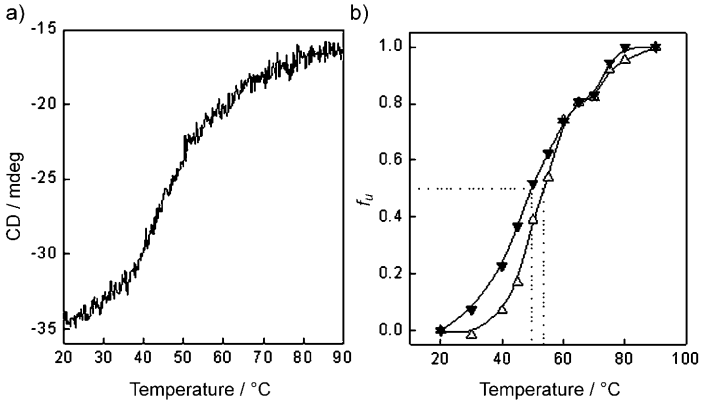

Figure 9. Thermal denaturation profiles of an equimolar mixture of DHAK and FBPA. a) Dichroism at $\lambda = 222$ nm and b) variation of the fraction of unfolding (▼) with temperature. The denaturation profile of DLF (△) is included for comparative purposes.

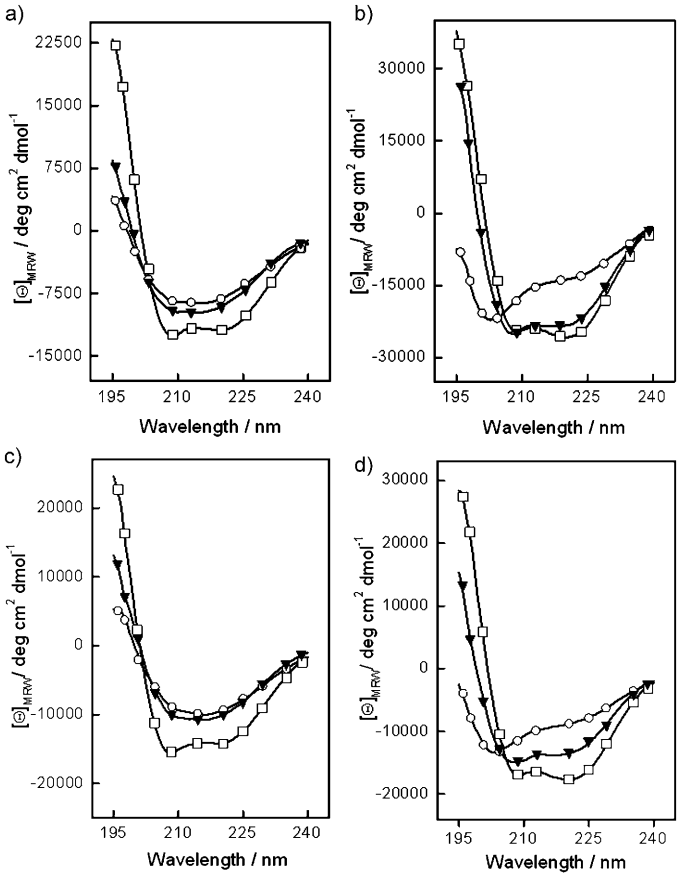

Figure 10. CD spectra at 20°C (□), 90°C (○), and again at 20°C after cooling the sample from 90°C (▼) of a) DHAK, b) FBPA, c) DLF, and d) an equimolar mixture of DHAK and FBPA.

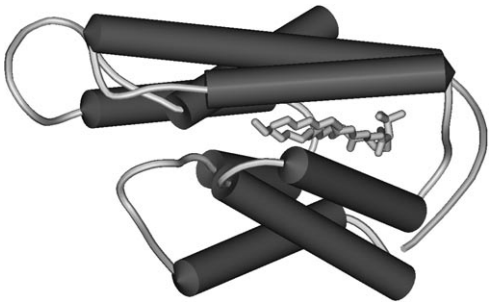

Figure 11. Crystallographic structure of the ATP binding domain from DHAK (pdb 1un9).[28] The phospholipid molecules that stabilize the folding are represented by sticks.

ferred, at least in part, to the fusion protein, thus making DLF a more thermostable biocatalyst than the multienzyme system.

However, the T_m value is directly related to conformational stability only if the unfolding is fully reversible. Irreversibility of the melting reaction is usually associated with protein precipitation or aggregation as it is unfolded. If this is the case, the melting temperature will not only depend on the intrinsic conformational stability but also on the kinetics of aggregation and the solubility of the unfolded form of the molecule. Only FBPA showed an almost complete recuperation (92%) of the secondary structure after denaturation at 90°C (Figure 10b). On the contrary, DHAK only recovered 51% of its original secondary structure (Figure 10a), thus showing that this protein tends to precipitate and/or aggregate after denaturing. This result can be explained by the particular structure of DHAK. This protein is a homodimer and each subunit is formed by two clearly differentiated domains.[28] The K domain is where the DHA binding site is located and the L domain bears the ATP binding site. The ATP binding domain is a barrel formed by eight amphipathic α-helices stabilized by a phospholipid molecule (Figure 11). The loss of this lipid after unfolding could explain the tendency of DHAK to aggregate. Once more, we could observe that the fusion was not neutral. Thus, the behavior of the equimolar mixture of DHAK and FBPA (Figure 10d) is practically the mean between DHAK and FBPA unfolding (the mixture recovered 70% of its original secondary structure). However, the fused enzyme DLF has a quite similar behavior to DHAK (Figure 10c) with an almost irreversible unfolding, although the percentage of the recovered original structure (54%) is slightly higher than the DHAK. This behavior indicates that unfolding of the DHAK domain dominates the thermotropic behavior of the full chimeric construct.

Finally, to analyze if the structural stability studied by CD spectroscopic analysis corresponded to the operational stability of the enzymes, we determine the functional half-life of the enzymes at 45°C (Figure 12).

To study how the fusion affected the activity of each enzyme, we independently evaluated the kinase and aldolase activities. DHAK, FBPA, and DLF were incubated at 45°C over time and their remnant activities were evaluated at room temperature. Therefore, we determined the progressive loss of activity due to irreversible denaturation of the enzymes in this assay. The results obtained in this experi-

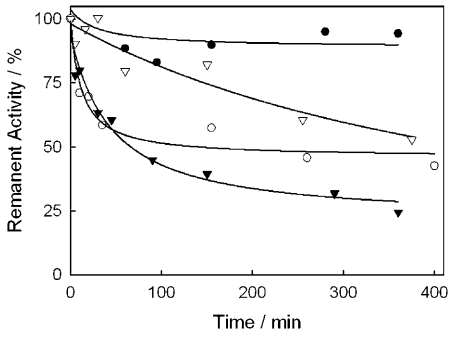

Figure 12. Operational stability at 45 °C of FBPA (●), DHAK (▼), aldolase activity of DLF (○), and kinase activity of DLF (▽).

ment were consistent with the results of the CD spectroscopic study. The half-life of the aldolase activity in the fused DLF decreased significantly with respect to the parent FBPA. This finding can be explained by the lower potential of renaturation of DLF with regards to FBPA. However, the half-life of the kinase activity significantly increased in the fusion enzyme with regard to the half-life of the parent DHAK. This increment could be due to the higher T_m value of the fusion enzyme.

In summary, although the aldolase activity is substantially destabilized relative to its parent enzyme, the kinase activity is markedly stabilized in the context of the fusion construct. Because the global thermal stability of both the multienzyme system and the fused DLF is determined by the less stable of their components, DLF should be considered to be a more thermostable biocatalyst than the multienzyme system; the half-life of its less-stable component (140 min for the aldolase activity) is more than double than the half-life of DHAK (65 min), the least-stable component of the multienzyme system.

Substrate channeling: A very interesting effect of the fusion of enzymes that work sequentially is an increase in their catalytic efficiency due to the proximity of the active centers in these covalently linked multienzyme complexes (see above).

Effectively, the overall rate of the coupled reaction catalyzed by the fused DLF was 0.41 μmol min^{-1}, whereas the overall rate was only 0.02 μmol min^{-1} with the multienzyme system. That is, the physical association of the enzymes produces a 20-fold increase in the aldol reaction rate.[27] This increase in the reaction rate could be explained in terms of substrate channeling. In the case of two free enzymes that work sequentially, the product of the first reaction must diffuse through the bulk solution to meet the second enzyme. In the fusion enzyme, the intermediate is directly transferred to the second enzyme without full diffusion and equilibration within the bulk solution. Therefore, DHAP produced by the kinase should have a lower transit time[36] to the aldolase active sites in the fusion enzyme relative to the multienzyme system, because the distance between the active centers has been significantly decreased. Alternatively, the obtained results can be explained from an increased local concentration of the intermediate DHAP in the proximity of the aldolase active center, thus producing, as a consequence, a concomitant increase in the reaction rate. In both cases, free diffusion of DHAP into the bulk solution is limited.

The possible occurrence of substrate channeling can be assessed by addition of a third enzyme, which could trap the intermediate, to the system. The activity of this third enzyme should be higher if the intermediate diffuses freely into the bulk solution rather than the case in which diffusion of the intermediate is limited (Scheme 4).

We carried out this experiment with glycerol-3-phosphate dehydrogenase (GDH) as the trapping enzyme. GDH catalyzes the reversible reduction of DHAP to glycerol-3-phosphate with concomitant oxidation of NADH (Scheme 4a). The GDH activity measured in the presence of the fused DLF enzyme or the multienzyme system formed by the parental free enzymes was significantly different (Figure 13).

In the presence of the fusion enzyme, the maximum GDH activity measured was 0.036 U with 10 μg of enzyme. With

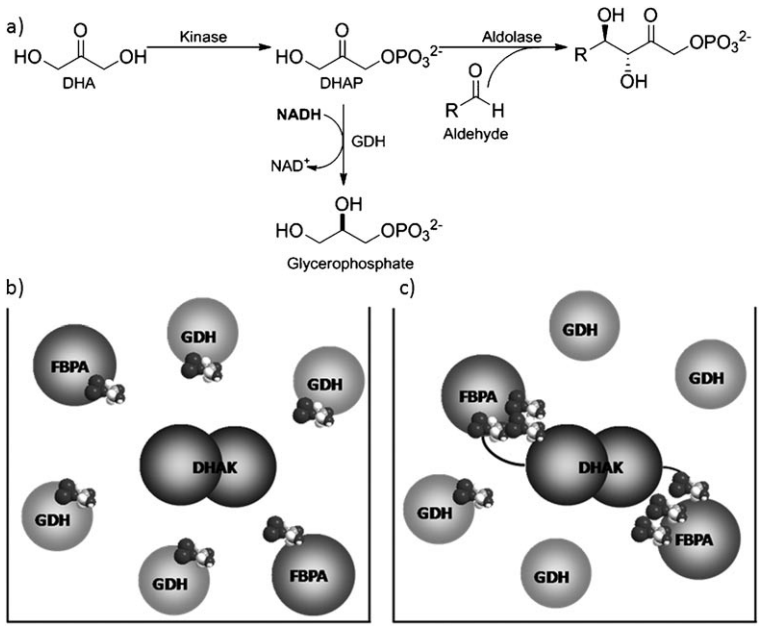

Scheme 4. GDH catalyzes the reduction of DHAP to glycerophosphate (a). In the multienzyme system in which DHAP can freely diffuse into the bulk solution (b), the GDH activity measured must be higher than in the presence of the fusion enzyme (c) in which DHAP is directly transferred to the aldolase without exposure to the bulk solution.

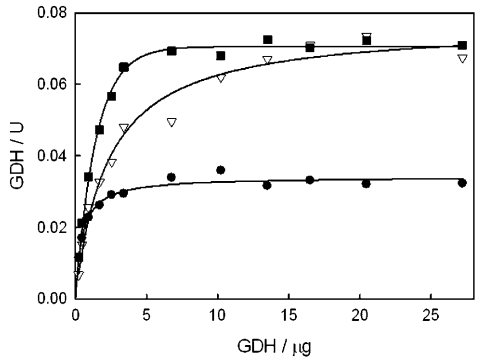

Figure 13. GDH activity measured in presence of the fused DLF enzyme (●) or in presence of the multienzyme system (▽). The third curve (■) represents the GDH activity measured in the presence of nonfunctional DLF because the acceptor aldehyde was not included in the reaction mixture.

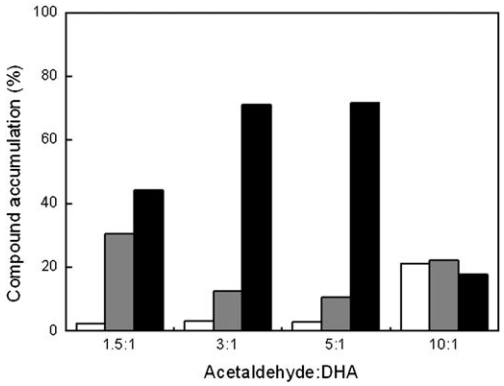

Figure 14. Accumulation of DHA (□), DHAP (■), and aldol adduct (■) in the reaction mixture at different acetaldehyde/DHA ratios.

this same amount of GDH, the activity measured in the presence of the multienzyme system was almost twice that (0.062 U). This result indicated that GDH had more substrate (DHAP) available with the multienzyme system than with the fusion enzyme. To confirm this interpretation, we measured the GDH activity in the presence of the fusion enzyme, but without adding the aldehyde acceptor. As a consequence, the second reaction catalyzed by DLF—the aldol addition reaction—is unviable, thus permitting DHAP to freely diffuse into the bulk solution. Under these conditions, the measured GDH activity reached similar values as in the presence of the multienzyme system (Figure 13), thus confirming the existence of the proposed channeling of DHAP in the fusion enzyme.

Synthetic applicability of DLF: One of the key features to ensure that the multienzyme system for the one-pot C–C bond formation previously described by us[17] operates optimally is that DHAP must be produced at the same rate as it is consumed by the aldolase to avoid its accumulation and to minimize its non-enzymatic degradation. Therefore, a delicate adjustment of the aldolase/kinase activity ratio was necessary. However, this adjustment is not possible when DLF is used because the ratio of kinase/aldolase (i.e., 1:3) is structurally fixed in the fusion enzyme. We explored whether a similar effect could be achieved by modulating the ketone/aldehyde ratio. We carried out this experiment with acetaldehyde **2** as an acceptor. In a first attempt, we used an acetaldehyde/DHA ratio of 1.5:1 equivalents. When the reaction was carried out with DLF (0.3 U of aldolase and 0.1 U of kinase), DHA had been almost completely consumed after 22 h, but only 28% of aldol could be detected. On the other hand, there was considerable accumulation of DHAP (37%). That is, about the 35% of the produced DHAP had been degraded during the reaction without giving place to aldol formation. By doubling the amount of enzyme, we got an increase in aldol formation that reached the 44%, thus decreasing the accumulation of DHAP to 30.6% (Figure 14).

With the highest acetaldehyde/DHA ratio (i.e., 10:1), it was observed that the ATP regeneration system did not work properly because as much as 21% of DHA remained after 22 hours without undergoing reaction. Under these conditions, the aldol formation was very poor and only reached less than 20%. On the other hand, the results obtained with the ratios 3:1 and 5:1 were very similar. In both cases, DHA was consumed almost completely – the ATP regeneration system works correctly. The accumulation of DHAP ranged between 10 and 12% and the formation of the aldol adduct reached 70% (Figure 14); that is, we could significantly increase the efficiency of the system by modulating the aldehyde/ketone ratio. For subsequent studies, we fixed the ratio at 3:1.

Once the optimum aldehyde/ketone ratio had been determined, we studied the synthetic applicability of DLF with benzyloxyacetaldehyde (**1**), acetaldehyde (**2**), and 3-(methylthio)propionaldehyde (**3**) as acceptors (Scheme 5).[27] These reactions were conducted on small scale with increased amounts of DLF relative to the previous experiments (1.35 U of aldolase and 0.45 U of kinase). The percentages of the aldol adducts obtained after reaction for 20 h were 58.2, 82.6, and 67.3% for **1**–**3**, respectively. Once more, an increase in the amount of DLF led to an improvement in the yield of the aldol formation, as observed for **5**, in which the yield increased from 70 to >80%.

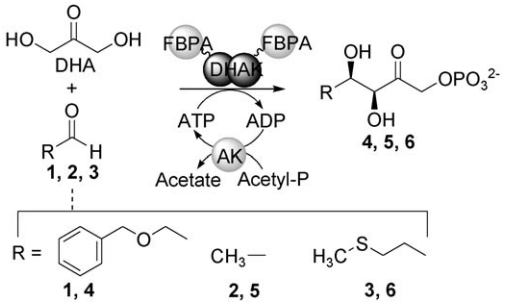

Scheme 5. Application of DLF to stereoselective C–C bond formation.

In a first attempt to determine if the stereoselectivity of the aldol reaction had been modified by the fusion process, we analyzed the stereoisomers formed in the DLF-catalyzed reactions by applying the enzymatic assay described by Sheldon and co-workers based on the reversibility of the aldol reaction.[37] In general, the results summarized in Table 3 are

Table 3. Stereoisomeric ratio of products formed in DLF-catalyzed reactions.[a]

Acceptor	Stereoisomer [%][b]		
	D-*threo*	L-*threo*	D-*erythro*
1	79.4	2.1	18.5
2	71.8	2.0	26.2
3	96.0	0	4.0

[a] Only stereoisomers with D-*threo*, L-*threo*, and D-*erythro* configurations could be detected. [b] The percentages were calculated with respect to the total aldol adduct formed.

in agreement with those reported by Sheldon and co-workers for FBPA from *S. carnosus*. In particular, the data regarding acetaldehyde **2** are not dissimilar to those data reported for the same aldehyde by Sheldon and co-workers.[37] However, the relatively high percentage of the D-*erythro* enantiomer obtained can be biased by some base-catalyzed epimerization at the C3 stereocenter due to the slightly alkaline pH value (pH 7.5) of the phosphate buffer used in this study. In summary, the aldol reaction catalyzed by DLF is highly, but far from absolutely, stereospecific for products with a D-*threo* configuration, and this reaction is strongly influenced by the acceptor. Nevertheless, we can conclude that the fusion process does not influence the stereoselectivity of the aldol reaction.

Conclusion

As part of our ongoing project on the development of more efficient and affordable biocatalysts for C–C bond-formation processes, we have engineered a bifunctional enzyme capable of catalyzing aldol addition reactions by using DHA as an initial ketone donor. This fusion enzyme, named DLF, consists of monomeric fructose-1,6-bisphosphate aldolase from *S. carnosus* and the homodimeric dihydroxyacetone kinase from *C. freundii* CECT 4626 with an intervening linker of five amino acids. The fusion protein was expressed soluble and retained both kinase and aldolase activities with a high catalytic efficiency (k_{cat}/K_M) on the order of 10^6 ($s^{-1}\,M^{-1}$). The CD spectroscopic study described herein has shown that the fusion of the parent enzymes only slightly affects the folding of the fused DLF enzyme. However, the renaturation capacity of DLF is lower than expected for an equimolar mixture of the parent enzymes. These results could be explained because a big protein such as *C. freundii* DHAK (over 120 kDa) may disturb the folding of FBPA (35 kDa), moreover, because FBPA is translated after DHAK.[38] The covalent union of both enzymes also allows some of their properties to be transferred to the fusion protein. Thus, the T_m value of the fused enzyme is almost identical to that of FBPA and is higher than would be expected if the fusion did not exercise any effect. On the other hand, we have demonstrated that the operational stability of the DLF enzyme is higher than that of the multienzyme system. We have also shown that the physical association of the parent enzymes produces an increase in the aldol reaction rate of 20-fold, which can be interpreted in terms of substrate channeling provided by the proximity of the active centers in the fusion enzyme. Finally, it seems that the fusion did not modify the steric course of the aldol reaction catalyzed by the bifuctional DLF enzyme.

In summary, with the described strategy we have been able to develop more affordable biocatalysts, which are more stable and efficient than the multienzyme system composed of the free parent enzymes. Work is in progress in our laboratories to apply this strategy to other DHAP-dependent aldolases.

Experimental Section

Materials and general procedures: *Staphylococcus carnosus* CECT 4491 was provided from the Spanish Type Culture Collection (CECT). *E. coli* BL21(DE3) competent cells were purchased from Stratagene Co. (San Diego, CA, USA). Restriction enzymes, Taq polymerase, and T4-DNA ligase were purchased from MBI Fermentas AB (Lithuania). Triosephosphate isomerase (TIM), α-glycerophosphate dehydrogenase (GDH), lysostaphin, and acetate kinase (AK) were purchased from Sigma–Aldrich (St. Louis, MO, USA). PCR primers were purchased from Isogen Life Science (Spain) and the pET-28b(+) expression vector was purchased from Novagen (Beeston, Nottingham, UK). Isopropyl-β-D-thiogalactopyranoside (IPTG) was purchased from Applichem GmBH (Germany). Plasmids and PCR purification kits were from Promega (Madison, WI, USA) and the DNA purification kit from agarose gels was from Eppendorf (Hamburg, Germany). SDS—PAGE was performed using 10 and 5% acrylamide in the resolving and stacking gels, respectively. Gels were stained with Coomassie brilliant blue R-250 (Applichem GmBH, Germany). Electrophoresis was always run under reducing conditions in the presence of 5% β-mercaptoethanol. Protein and DNA gels were quantified by densitometry using GeneGenius Gel Documentation and Analysis System (Syngene, U.K.). Nickel/iminodiacetic acid (Ni^{2+}/IDA) agarose was supplied by Agarose Bead Technologies (Spain). Size-exclusion chromatography was carried out on a HiLoad 26/60 Superdex 75 PG column controlled with the AKTA-FPLC system (GE Healthcare Life Science). ^1H and ^{13}C NMR spectra were recorded with D_2O as the solvent on a Varian system 500 spectrometer equipped with a 5-mm HCN cold probe with field *z* gradient operating at 500.13 and 125.76 MHz for the ^1H and ^{13}C NMR spectra, respectively. The sample temperature was maintained constantly at 298 K. One-dimensional NMR experiments were performed using standard Varian pulse sequences. Two-dimensional [^1H, ^1H] NMR experiments (gCOSY) were carried out with the following parameters: a delay time of 1 s, a spectral width of 3000 Hz in both dimensions, 4096 complex points in *t*2 and *t*4 transients for each of 256 time increments, and a linear prediction to 512. The data were zero-filled to 4096×4096 real points. Two-dimensional [^1H, ^{13}C] NMR experiments (gHSQC and gHMBC) used the same ^1H NMR spectral window, a ^{13}C NMR spectral windows of 15 000 Hz, 1-s relaxation delay, 1024 data points, and 256 time increments with a linear prediction to 512. The data were zero-filled to 4096×4096 real points. Typical numbers of transients per increment were 4 and 16, respectively.

Cloning, over-expression, and purification of FBPA from *S. Carnosus*: DNA manipulation was carried out according to standard procedures.[39]

The DNA template for the amplification of the *fda* gene was obtained from the *S. carnosus* strain CECT 4491. The oligonucleotides 5′-ATATTCATATGAACCAAGAACAACAATTTGAC-3′ and 5′-TATTACTCGAGTTAAGCTTTGTTTACTGA-3′ were used as leftward and rightward primers, respectively (the recognition sequence for *Nde*I and *Xho*I are underlined). To extract the DNA, *S. carnosus* cells was suspended in lysis buffer containing tris(hydroxymethyl)aminomethane (Tris) 10 mM, ethylenediaminetetraacetic acid (EDTA) 10 mM, lysozyme (200 U mL^{-1}), and lysostaphin (25 U mL^{-1}).[40] PCR amplification was performed in a 10-μL reaction mixture and subjected to 25 cycles of amplification. The cycle conditions were set as follows: denaturation at 94 °C for 1 min, annealing at 55 °C for 2 min, and elongation at 72 °C for 1 min. The purified PCR product was digested with *Nde*I and *Xho*I and ligated into the doubled digested vector pET-28b(+) to yield the plasmid pET-*fda*. This plasmid was transformed into *E. coli* BL21(DE3) competent cells. A colony containing the plasmid pET-*fda* was cultured in Luria-Bertani (LB) broth containing kanamycin (26 μg mL^{-1}) at 37 °C with shaking. When the culture reached an optical density value at $\lambda = 600$ nm ($OD_{600\,nm}$) of 0.5–0.6, FBPA expression was induced with IPTG (0.4 mM) and the temperature was decreased to 30 °C. The culture was maintained overnight, after which the culture was centrifuged at 3000 × *g* over 30 min at 4 °C, and the resulting pellet was treated with lysozyme and DNase for protein extraction.[41] The recombinant protein containing an N-terminal 6× histidine tag was purified on a Ni^{+2}/IDA agarose column preequilibrated with sodium phosphate buffer (20 mM, pH 7.5). FBPA was eluted with the same buffer containing imidazole (1 M). All the fractions containing protein were pooled together and further purified by size-exclusion chromatography on a HiLoad 26/60 Superdex 75 PG column controlled by the AKTA-FPLC system (GE Healthcare Life Science). The column was developed in phosphate buffer (50 mM, pH 7.2) containing NaCl (0.15 M) at a constant flow rate of 1.0 mL min^{-1}

Construction, expression, and purification of the bifuctional DLF enzyme: The *dhak-l-fda* fusion gene was constructed by gene splicing through overlap extension.[33] The sequences of the primers used are shown in Table 4.

The first two PCR amplifications were performed in 10 μL of reaction mixture and subjected to 25 cycles of amplification. The cycle conditions were: denaturation at 94 °C for 1 min, annealing at 55 °C for 1 min, and elongation at 72 °C for 2 min. A 1:1 mixture of the purified PCR products was used as the template in the second PCR step. The reaction conditions were identical to those previously described, except for an elongation time of 3 min. After purification, the *dhak-l-fda* fragment was digested with *Nde*I and *Xho*I and ligated into the doubled digested vector pET-28b(+) to yield the plasmid pET-*dhak-l-fda*. This plasmid was transformed into *E. coli* BL21(DE3) competent cells. The procedures for the expression and purification of the bifuctional enzyme were identical to the procedure described for the FBPA enzyme, except in the IMAC purification step. In this case, the column was washed with sodium phosphate buffer (10×, 20 mM, pH 7.5) containing imidazole 50 mM prior to eluting the enzyme with imidazole (1 M).

Protein analysis: Amino acid analysis of purified recombinant proteins was performed at the Protein Chemistry Service of the Centre of Biological Research (CIB-CSIC, Spain) to determine the protein concentration. The absorption spectrum of different quantified samples allowed the determination of the molar extinction coefficient at $\lambda = 280$ nm for recombinant FBPA ($\varepsilon^{280} = 46\,292\ M^{-1}cm^{-1}$) and for DLF ($\varepsilon^{280} = 77\,928\ M^{-1}cm^{-1}$). Peptide-mass fingerprint analyses from the SDS–PAGE band that correspond to the putative FBPA and DLF were performed at the Proteomic Unit of the Spanish National Center of Biotechnology (CNB-CSIC). The samples were digested with sequencing-grade trypsin overnight at 37 °C. The analysis by MALDI-TOF mass-spectrometric analysis produces peptide-mass fingerprints and the peptides observed can be collated and represented as a list of monoisotopic molecular weights. The data were collected in the range *m/z* 800–3600. Sedimentation equilibrium experiments were performed at the Department of Chemical Physics of Biological Macromolecules (Institute of Chemical Physics "Rocasolano"; CSIC). The initial concentration of the protein used in these experiments was 0.96 mg mL^{-1}.

Circular dichroism (CD) studies: Far-UV circular dichroism (CD) spectra were recorded in the range $\lambda = 195$–240 nm on a Jasco J-810 spectropolarimeter equipped with a constant temperature cell-holder Jasco PTC423-S Peltier. The protein concentration was 0.2–0.4 mg mL^{-1} (3.1–6.2 μM) for DHAK, 0.1–0.2 mg mL^{-1} (2.9–5.8 μM) for FBPA, and 0.6–0.7 mg mL^{-1} (6.4–7.5 μM) for DLF. The optical path length was 0.1 cm. The contribution of the buffer was always subtracted. For each sample, four spectra were accumulated at a scan speed of 20 nm min^{-1} with a bandwidth of 0.2 nm and averaged automatically. The mean residue ellipticity $[\Theta]$ is given in units of deg cm^2 dmol^{-1}. The secondary structure of the protein was evaluated by a computer fit of the CD spectrum into four simple components (α-helix, β-sheet, turns, and random coil) by using the CDPro software package containing three commonly used programs: SELCON3, CONTIN/LL, and CDSSTR (see Figures S1 and S2 in the Supporting Information).[42] This software allows the use of different sets of proteins to increase the reliability of the analyses. We choose the set number four, composed of 43 soluble proteins. From data obtained for DHAK and FBPA, the theoretical structural composition of an equimolar mixture was calculated by applying Equation (1):

$$\psi_M = \frac{\psi_{DHAK} PM_{DHAK} + \psi_{FBPA} PM_{FBPA}}{PM_M} \quad (1)$$

where ψ is each secondary structure (α-helix, β-sheet, turns, or random coil) and PM is the molecular weight of the corresponding protein.

The thermal stability was assessed by following changes in the entire spectrum in the far-UV CD region with increasing temperature from 20 to 90 °C (see Figure S3 in the Supporting Information). Thermal transition curves were obtained by monitoring the DC signal at $\lambda = 222$ nm as a function of the temperature. The temperature gradient was 40 °C h^{-1} and the data were recorded every 0.2 °C. These curves were fitted to a simple thermodynamic unfolding model [Eq. (2)]:

$$Y = (D_0 + m_D X) - \frac{(D_0 - N_0) + (m_D - m_N)X}{1 + \exp\frac{H_D(X - T_M)}{1.98(273.15+X)(273.15+T_M)}} \quad (2)$$

where D_0 is the value of the DC signal (mdeg) of the unfolded state at $T = 0$ °C; m_D is the slope of the unfolded state; N_0 is the value of the DC signal (mdeg) of the native state at $T = 0$ °C; m_N is the slope of the native state; T_M is the temperature (°C) of the inflection point, and H_D is the van't Hoff enthalpy associated to the denaturation process at $T = T_M$.

The fraction of unfolding f_u at each temperature was calculated by dividing the amount of α-helix lost from the folded state by the total loss of α-helix [Eq. (3)].

$$f_u = (h_n - h_T)/(h_n - h_u) \quad (3)$$

where h_T is the normalized content of α-helix at a given temperature and h_n and h_u are the normalized content of α-helix in the folded and unfolded states, respectively.

Table 4. Sequences of the primers used to splice the *dhak* and *fda* genes.[a]

Fragment	Primer	Sequence
dhak-l	NtNdhak[b]	5′-ATATT**CATATG**TCTCAATTCTTTTTT-3′
	CtFdhak	5′-CTGGCCCTGGCCCTGGCCCAGCTCACTCTC-3′
l-fda	CtScXfda[c]	5′-TATTA**CTCGAG**TTAAGCTTTGTTTACTGA-3′
	NtFScfda	5′-CAGGGCCAGGGCCAGAACCAAGAACAATTTGACAAA-3′
dhak-l-fda	NtNdhak[b]	5′-ATATT**CATATG**TCTCAATTCTTTTTT-3′
	CtScXfda[c]	5′-TATTA**CTCGAG**TTAAGCTTTGTTTACTGA-3′

[a] The endonuclease recognition sequences are in bold and the linker sequence are underlined. [b] Restriction enzyme *Nde*I. [c] Restriction enzyme *Xho*I.

Enzyme activity assays and steady-state kinetic analysis: Phosphorylation of DHA was measured spectrophotometrically in a coupled enzymatic assay as previously described.[18] Aldolase activity was spectrophotometrically measured by the retro-aldol reaction using fructose-1,6-bisphosphate (FBP) as the substrate.[43] The aldolase activity assays were run at room temperature by following the decrease in absorbance at $\lambda = 340$ nm ($\varepsilon_{NADH} = 6220\,M^{-1}cm^{-1}$) for 5 min in the reaction mixture (1 mL) containing Tris-HCl buffer (40 mM, pH 8.0), nicotinamide adenine dinucleotide (NADH; 0.2 μmol), α-glycerol phosphate dehydrogenase/triose phosphate isomerase (α-GDH/TIM; 2 U), FBP (1.0 μmol), and fructose-1,6-bisphosphate aldolase (FBPA) or the bifunctional DLF. Steady-state kinetic assays with DLF were measured at 25 °C in 96-well plates in a total volume of 0.3 mL. The measurements of the kinetic parameters for FBP were performed with 5.3 $\mu g\,mL^{-1}$ of purified protein at sixteen different FBP concentrations in the range 0.005–0.25 mM. Assays to determine the kinetic parameters for DHA were performed with 24 $\mu g\,mL^{-1}$ of purified DLF at twelve concentrations of substrate under saturating concentrations of $[Mg–ATP]^{2-}$ complex (3.75 mM). Steady-state kinetic assays with FBPA were carried out as well at 25 °C in 96-well plates in a total volume of 0.3 mL. Measurements of the kinetic parameters for FBP were performed with 0.83 $\mu g\,mL^{-1}$ of purified protein at twenty different FBP concentrations in the range 0.005–0.6 mM. Kinetic constants were obtained by using the built-in nonlinear regression tools in SigmaPlot 8.0. For the determination of apparent kinetic constants (variation of only one substrate), initial velocities V_i were fitted to the Michaelis–Menten equation.

Substrate channeling assay: To study the possible substrate channeling promoted by the proximity of the active centers in the fused enzyme, the rates of the coupled reaction catalyzed by DLF or a combination of the two parent enzymes were measured and compared under the same conditions. In both cases, 0.91 U of kinase activity and 2.66 U of aldolase activity were used. It was necessary to use a slightly greater amount of DLF in terms of milligrams of protein to fit the units of activity. Thus, 0.49 mg of DLF was used by a total of 0.175 mg of DHAK (0.114 mg) and FBPA (0.061 mg). The reactions were carried out at room temperature in phosphate buffer (1.5 mL, 20 mM, pH 7.5) containing DHA (0.05 mmol), benzyloxyacetaldehyde (**1**; 0.15 mmol), $MgSO_4$ (12.5 μmol), and ATP (12.5 μmol). At different times, aliquots (50 μL) were taken. The reaction was stopped with $HClO_4$ (7%), and the aldol product formed quantified by the retro-aldol assay. In the DHAP trapping experiment, GDH activity was measured in competition with the coupled reactions catalyzed by DLF or by the multienzyme system. GDH activity was measured spectrophotometrically by following the decrease in absorbance at $\lambda = 340$ nm due to oxidation by NADH for 10 min. In all cases, 0.04 U of kinase activity and 0.12 U of aldolase activity were used. The reactions were carried out at room temperature in phosphate buffer (1 mL, 20 mM, pH 7.5) containing DHA (2.5 μmol), acetaldehyde (**2**; 7.5 μmol), $MgSO_4$ (5 μmol), NADH (0.2 μmol), ATP (3.75 μmol), and different amounts of GDH in the range 0.231–33.99 μg.

Synthetic application of the bifunctional DLF enzyme: The C–C bond-formation reactions catalyzed by the fusion enzyme DLF were carried out at room temperature in phosphate buffer (1.5 mL, 20 mM, pH 7.5) containing DHA (0.05 mmol), aldehyde acceptor (0.15 mmol; **1**, **2**, and **3**, respectively), acetyl phosphate (0.1 mmol), $MgSO_4$ (12.5 μmol), AK (3 U), and DLF (1.5–2 U and 3–6 U of kinase and aldolase activities, respectively). The reactions started with the addition of ATP (3.4 μmol). When the consumption of DHA was greater than 90% (~20 h), the reactions were stopped and passed through activated carbon. The eluent was freeze-dried for NMR spectroscopic characterization. The determination of the stereoisomeric products formed by bifuctional DLF was carried out following the method described by Sheldon and co-workers.[37]

5-(Benzyloxy)-3,4-dihydroxy-2-oxopentyl phosphate (4): ^{1}H NMR (500 MHz, D_2O, 298 K): $\delta = 7.2$–7.1 (m, 5H, Ar), 4.52 (dd, 1H, $J = 18.5$, 5.8 Hz, H1A), 4.40 (dd, 1H, $J = 18.5$, 5.8 Hz, H1B), 4.4–4.3 (m, 2H, CH_2Ph), 4.29 (s, 1H, H3), 4.15–4.05 (m, 1H, H4), 3.50–3.45 (m, 1H, H5A), 3.45–3.40 ppm (m, 1H, H5B); ^{13}C NMR (125 MHz, D_2O, 298 K): $\delta = 212.3$ (C2), 129.5 (Ar), 129.3 (Ar), 128.9 (Ar), 128.6 (Ar), 75.5 (C1), 73.1 (C5), 72.4 (CH_2Ph), 70.5 (C4), 70.2 ppm (C3).

3,4-Dihydroxy-2-oxopentyl phosphate (5): ^{1}H NMR (500 MHz, D_2O, 298 K): $\delta = 4.55$ (dd, 1H, $J = 18.8$, 6.1 Hz, H1A), 4.45 (dd, 1H, $J = 18.8$, 6.1 Hz, H1B), 4.20 (d, 1H, $J = 2.6$ Hz, H3), 4.14 (dq, 1H, $J = 6.4$, 2.4 Hz, H4), 1.10 ppm (d, 3H, $J = 6.3$ Hz, Me); ^{13}C NMR (125 MHz, D_2O, 298 K): $\delta = 211.6$ (C2), 78.5 (C3), 67.9 (C4), 67.7 (C1), 18.4 ppm (Me).

3,4-Dihydroxy-6-(methylthio)-2-oxohexyl phosphate (6): ^{1}H NMR (500 MHz, D_2O, 298 K): $\delta = 4.55$ (dd, 1H, $J = 18.8$, 6.6 Hz, H1A), 4.45 (dd, 1H, $J = 18.8$, 6.6 Hz, H1B), 4.28 (d, 1H, $J = 2.2$ Hz, H3), 4.05 (ddd, 1H, $J = 14.4$, 11.5, 9.2 Hz, H4), 2.5–2.4 (m, 2H, H6), 1.95 (s, 3H, Me), 1.8–1.7 ppm (m, 2H, H5); ^{13}C NMR (125 MHz, D_2O, 298 K): $\delta = 211.5$ (C2), 77.7 (C3), 70.4 (C4), 68.1 (C1), 29.6 (C6), 23.5 (C5), 14.3 ppm (Me).

Acknowledgements

We thank the Spanish Ministerio de Ciencia e Innovación for financial support (Grant CTQ2007-67403/BQU). J.P.-G. has been supported by grants BIO2009-09694 and CSD2007-00010. L.I. and I.S.-M. acknowledge the Predoctoral Fellowship from Comunidad de Madrid. I.O.-G. is a JAE-Predoc fellow from CSIC. We thank E. G. Doyagüez for her assistance on NMR spectroscopic characterization.

[1] a) C. J. Li, *Chem. Rev.* **2005**, *105*, 3095–3166; b) *Modern Aldol Reactions, Vol. 1* (Ed.: R. Mahrwald), Wiley-VCH, Weinheim, **2004**; *Modern Aldol Reactions, Vol. 2* (Ed.: R. Mahrwald), Wiley-VCH, Weinheim, **2004**; c) C. Palomo, M. Oiarbide, J. M. García, *Chem. Soc. Rev.* **2004**, *33*, 65–75; d) B. Alcaide, P. Almendros, *Angew. Chem.* **2003**, *115*, 884–886; *Angew. Chem. Int. Ed.* **2003**, *42*, 858–860.

[2] For some recent reviews, see: a) L. Hecquet, V. Helaine, F. Charmantray, M. Lemaire in *Modern Biocatalysis: Stereoselective and Environmentally Friendly Reactions* (Eds.: W.-D. Fessner, T. Anthonsen), Wiley-VCH, Weinheim, **2009**, pp. 287–298; b) P. Clapes, G. A. Sprenger, J. Joglar in *Modern Biocatalysis: Stereoselective and Environmentally Friendly Reactions* (Eds.: W.-D. Fessner, T. Anthonsen), Wiley-VCH, Weinheim, **2009**, pp. 299–306; c) L. Iturrate, E. García-Junceda in *Multi-Step Enzyme Catalysis: Biotransformations and Chemoenzymatic Synthesis* (Ed.: E. García-Junceda), Wiley-VCH, Weinheim, **2008**, pp. 61–81; d) W.-D. Fessner in *Asymmetric Organic Synthesis with Enzymes* (Eds.: V. Gotor, I. Alfonso, E. García-Urdiales), Wiley-VCH, Weinheim, **2008**, pp. 275–318; e) A. K. Samland, G. A. Sprenger, *Appl. Microbiol. Biotechnol.* **2006**, *71*, 253–264; f) L. J. Whalen, C.-H. Wong, *Aldrichimica Acta* **2006**, *39*, 63–71; g) J. Sukumaran, U. Hanefeld, *Chem. Soc. Rev.* **2005**, *34*, 530–542.

[3] a) D. G. Drueckhammer, J. R. Durrwachter, R. L. Pederson, D. C. Crans, L. Daniels, C.-H. Wong, *J. Org. Chem.* **1989**, *54*, 70–77; b) R. Schoevaart, F. Van Rantwijk, R. A. Sheldon, *J. Org. Chem.* **2001**, *66*, 4559–4562; c) M. Sugiyama, Z. Hong, L. J. Whalen, W. A. Greenberg, C.-H. Wong, *Adv. Synth. Catal.* **2006**, *348*, 2555–2559.

[4] M. Sugiyama, Z. Hong, W. A. Greenberg, C.-H. Wong, *Bioorg. Med. Chem.* **2007**, *15*, 5905–5911.

[5] a) J. Wagner, R. A. Lerner, C. F. Barbas III, *Science* **1995**, *270*, 1797–1800; b) C. F. Barbas III, A. Heine, G. Zhong, T. Hoffmann, S. Gramatikova, R. Björnestedt, B. List, J. Anderson, E. A. Stura, I. A. Wilson, R. A. Lerner, *Science* **1996**, *271–274*, 2085–2092; c) J.-L. Reymond, *J. Mol. Cat. B* **1998**, *5*, 331–337; d) F. Tanaka, R. Fuller, C. F. Barbas III, *Biochemistry* **2005**, *44*, 7583–7592.

[6] L. Jiang, E. A. Althoff, F. R. Clemente, L. Doyle, D. Rothlisberger, A. Zanghellini, J. L. Gallaher, J. L. Betker, F. Tanaka, C. F. Barbas III, D. Hilvert, K. N. Houk, B. L. Stoddard, D. Baker, *Science* **2008**, *319*, 1387–1391.

[7] a) M. Schurmann, G. A. Sprenger, *J. Biol. Chem.* **2001**, *276*, 11055–11061; b) M. Schürmann, M. Schürmann, G. A. Sprenger, *J. Mol. Catal. B* **2002**, *19–20*, 247–252; c) J. A. Castillo, J. Calveras, J. Casas, M. Mitjans, M. P. Vinardell, T. Parella, T. Inoue, G. A. Sprenger, J.

Joglar, P. Clapés, *Org. Lett.* **2006**, *8*, 6067–6070; d) M. Sugiyama, Z. Hong, P. H. Liang, S. M. Dean, L. J. Whalen, W. A. Greenberg, C.-H. Wong, *J. Am. Chem. Soc.* **2007**, *129*, 14811–14817; e) X. Garrabou, J. A. Castillo, C. Guérard-Hélaine, T. Parella, J. Joglar, M. Lemaire, P. Clapés, *Angew. Chem.* **2009**, *121*, 5629–5633; *Angew. Chem. Int. Ed.* **2009**, *48*, 5521–5525.

[8] For an in-depth discussion of the chemical and enzymatic routes to DHAP, see: M. Schümperli, R. Pellaux, S. Panke, *Appl. Microbiol. Biotechnol.* **2007**, *75*, 33–45, and references therein.

[9] a) S. H. Jung, J.-H. Jeong, P. Miller, C.-H. Wong, *J. Org. Chem.* **1994**, *59*, 7182–7184; b) F. Charmantray, L. El Blidi, T. Gefflaut, L. Hecquet, J. Bolte, M. Lemaire, *J. Org. Chem.* **2004**, *69*, 9310–9312.

[10] T. Gefflaut, M. Lemaire, M.-L. Valentin, J. Bolte, *J. Org. Chem.* **1997**, *62*, 5920–5922.

[11] W. D. Fessner, G. Sinerius, *Angew. Chem.* **1994**, *106*, 217–220; *Angew. Chem. Int. Ed. Engl.* **1994**, *33*, 209–212.

[12] R. Schoevaart, F. van Rantwijk, R. A. Sheldon, *J. Org. Chem.* **2000**, *65*, 6940–6943.

[13] F. Charmantray, P. Dellis, S. Samreth, L. Hecquet, *Tetrahedron Lett.* **2006**, *47*, 3261–3263.

[14] T. van Herk, A. F. Hartog, H. E. Schoemaker, R. Wever, *J. Org. Chem.* **2006**, *71*, 6244–6247.

[15] C.-H. Wong, G. M. Whitesides, *J. Org. Chem.* **1983**, *48*, 3199–3205.

[16] N. Itoh, Y. Tujibata, J. Q. Liu, *Appl. Microbiol. Biotechnol.* **1999**, *51*, 193–200.

[17] a) I. Sánchez-Moreno, J. F. García-García, A. Bastida, E. García-Junceda, *Chem. Commun.* **2004**, 1634–1635; b) I. Sánchez-Moreno, L. Iturrate, E. G. Doyagüez, J. A. Martínez, A. Fernández-Mayoralas, E. García-Junceda, *Adv. Synth. Catal.* **2009**, *351*, 2967–2975.

[18] I. Sánchez-Moreno, L. Iturrate, R. Martín-Hoyos, M. L. Jimeno, M. Mena, A. Bastida, E. García-Junceda, *ChemBioChem* **2009**, *10*, 225–229.

[19] See special issue on "Bioseparation": *J. Chem. Technol. Biotechnol.* **2008**, *83*, (Ed.: M. Rito-Palomares), and references therein.

[20] a) L. Bülow, K. Mosbach, *Trends Biotechnol.* **1991**, *9*, 226–231; b) M. Uhlen, G. Forsberg, T. Moks, M. Hartmanis, B. Nilsson, *Curr. Opin. Biotechnol.* **1992**, *3*, 363–369; c) A. E. Nixon, M. Ostermeier, S. J. Benkovic, *Trends Biotechnol.* **1998**, *16*, 258–264.

[21] T. Mizuno, K. Murao, Y. Tanabe, M. Oda, T. Tanaka, *J. Am. Chem. Soc.* **2006**, *128*, 11378–11383.

[22] L. Tian, R. A. Dixon, *Planta* **2006**, *224*, 496–507.

[23] For some reviews, see: a) F. Trejo, J. L. Gelpi, M. Busquets, A. Cortes, *Curr. Top. Pept. Protein Res.* **1999**, *3*, 173–180; b) S. Stahl, S. Hober, J. Nilsson, M. Uhlen, P.-A. Hygren, *Biotechnol. Bioeng.* **2003**, *27*, 95–129; c) J. J. Lichty, J. L. Malecki, H. D. Agnew, D. J. Michelson-Horowitz, S. Tan, *Protein Expression Purif.* **2005**, *41*, 98–105.

[24] We adopt here the operational definition of substrate channeling given by Ovádi et al., according to which the term "substrate channeling" designates the coupling of two or more enzymatic reactions in which the reaction product of one enzyme is transferred to the next enzyme without escaping into the bulk phase; see: a) J. Ovádi, *J. Theor. Biol.* **1991**, *152*, 1–22; b) H. O. Spivey, J. Ovádi, *Methods* **1999**, *19*, 306–321.

[25] a) C. L. James, R. E. Viola, *Biochemistry* **2002**, *41*, 3720–3725; b) C. L. James, R. E. Viola, *Biochemistry* **2002**, *41*, 3726–3731.

[26] For some selected examples, see: a) P. Ljungcrantz, H. Carlsson, M. O. Mansson, P. Buckel, K. Mosbach, L. Bülow, *Biochemistry* **1989**, *28*, 8786–8792; b) P. Ljungcrantz, L. Bülow, K. Mosbach, *FEBS Lett.* **1990**, *275*, 91–94; c) Y. Tamada, B. A. Swanson, A. Arabshahi, P. A. Frey, *Bioconjugate Chem.* **1994**, *5*, 660–665; d) X. Chen, Z. Liu, J. Wang, J. Fang, H. Fan, P. G. Wang, *J. Biol. Chem.* **2000**, *275*, 31594–31600; e) Y. H. Khang, I. W. Kim, Y. R. Hah, J. H. Hwangbo, K. K. Kang, *Biotechnol. Bioeng.* **2003**, *82*, 480–488; f) Y. Zhang, S.-Z. Li, J. Li, X. Pan, R. E. Cahoon, J. G. Jaworski, X. Wang, J. M. Jez, F. Chen, O. Yu, *J. Am. Chem. Soc.* **2006**, *128*, 13030–13031; g) L. Tian, R. A. Dixon, *Planta* **2006**, *224*, 496–507; h) D. E. Torres Pazmiño, R. Snajdrova, B.-J. Baas, M. Ghobrial, M. D. Mihovilovic, M. W. Fraaije, *Angew. Chem.* **2008**, *120*, 2307–2310; *Angew. Chem. Int. Ed.* **2008**, *47*, 2275–2278.

[27] A preliminary account of this study has been reported in communication format: L. Iturrate, I. Sanchez-Moreno, E. G. Doyaguez, E. Garcia-Junceda, *Chem. Commun.* **2009**, 1721–1723.

[28] C. Siebold, I. Arnold, L. F. García-Alles, U. Baumann, B. Erni, *J. Biol. Chem.* **2003**, *278*, 48236–48244.

[29] a) H. P. Brockamp, M. R. Kula, *Appl. Microbiol. Biotechnol.* **1990**, *34*, 287–291; b) M. T. Zannetti, C. Walter, M. Knorst, W.-D. Fessner, *Chem. Eur. J.* **1999**, *5*, 1882–1890; c) M. Dinkelbach, M. Hodenius, A. Steigel, M. R. Kula, *Biocatal. Biotransform.* **2001**, *19*, 51–68.

[30] a) C. Witke, F. Götz, *J. Bacteriol.* **1992**, *174*, 7495–7499; b) Y. Kim, M. Zhou, S. Moy, A. Joachimiak, PDB: 2IQT.

[31] a) M. C. Peitsch, *Bio/Technology* **1995**, *13*, 658–660; b) K. Arnold, L. Bordoli, J. Kopp, T. Schwede, *Bioinformatics* **2005**, *22*, 195–201; c) F. Kiefer, K. Arnold, M. Künzli, L. Bordoli, T. Schwede, *Nucleic Acids Res.* **2009**, *37*, D387–D392.

[32] a) C. J. Crasto, J.-A. Feng, *Protein Eng.* **2000**, *13*, 309–312; b) F. Xue, Z. Gu, J.-A. Feng, *Nucleic Acids Res.* **2004**, *32*, W562-W565.

[33] R. M. Horton, H. D. Hunt, S. N. Ho, J. K. Pullen, L. R. Pease, *Gene* **1989**, *77*, 61–68.

[34] L. M. Mayr, O. Landt, U. Hahn, F. X. Schmidt, *J. Mol. Biol.* **1993**, *231*, 897–912.

[35] a) K.-P. Wong, C, Tanford, *J. Biol. Chem.* **1973**, *248*, 8518–8523; b) L. Z. Wu, B. L. Ma, D. W. Zou, Z. X. Tie, J. Wang, W. Wang, *J. Mol. Struct.* **2008**, *877*, 44–49.

[36] Transit time is the time required for a metabolite to reach the next enzyme in the pathway and is expected to be on the order of r^2_E/D_s, where r_E is the average separation distance of enzyme molecules and D_s is the diffusion coefficient of the substrate: G. R. Welch, *Prog. Biophys. Mol. Biol.* **1978**, *32*, 103–191.

[37] R. Schoevaart, F. van Rantwijk, R. A. Sheldon, *Biotechnol. Bioeng.* **2000**, *70*, 349–352.

[38] A. Stanislawska-Sachadyn, P. Sachadyn, K. Ihle, C. Sydorczuk, K. Wiejacha, J. Kur, *J. Biotechnol.* **2006**, *121*, 134–143.

[39] J. Sambrook, E. F. Fritsch, T. Maniatis, *Molecular Cloning: A laboratory Manual*, 2nd ed., Cold Spring Harbor Laboratory Press, Cold Spring Harbor, **1989**.

[40] M. Ligozzi, R. Fontana, *Afr. J. Biotechnol.* **2003**, *2*, 251–253.

[41] A. Bastida, A. Fernández-Mayoralas, R. Gómez, F. Iradier, J. C. Carretero, E. García-Junceda, *Chem. Eur. J.* **2001**, *7*, 2390–2397.

[42] N. Sreerama, R. W. Woody, *Anal. Biochem.* **2000**, *287*, 252–260.

[43] H. U. Bergmeyer, *Methods of Enzymatic Analysis, Vol. 2*, 3rd ed., VCH, Weinheim, **1984**.

Received: November 11, 2009
Published online: March 2, 2010

